

# AUTOSOMAL DOMINANT VITREORETINOCHOROIDOPATHY

## When Molecular Genetic Testing Helps Clinical Diagnosis

ELISE BOULANGER-SCEMAMA, MD,\* JOSE-ALAIN SAHEL, MD, PhD,\*†‡§¶|| SADDEK MOHAND-SAID, MD,†§ ALINE ANTONIO,§ CHRISTEL CONDROYER,§ CHRISTINA ZEITZ, PhD,§ ISABELLE AUDDO, MD, PhD†§\*\*

---

**Purpose:** Autosomal dominant vitreoretinopathies are an extremely rare disease, which belongs to the *BEST1*-related disease spectrum.

**Methods:** Report of five patients with an initial diagnosis of atypical rod-cone dystrophy, for whom autosomal dominant vitreoretinopathies was retrospectively diagnosed on genetic results using targeted next-generation sequencing. Each patient had a comprehensive ophthalmic examination including multimodal retinal imaging and functional evaluation.

**Results:** Visual acuity ranged from <20/800 to 20/25. Two patients had narrowed angle with history of acute angle-closure glaucoma for one patient. Full-field electroretinogram showed severe reduction of both scotopic and photopic responses for 3/5 patients. Electrooculogram could be performed for one of the two patients with moderate alterations of full-field electroretinogram. It revealed severe light rise abnormalities with decreased Arden ratio (125% right eye, 145% left eye) in keeping with generalized severe dysfunction of the retinal pigment epithelium. On funduscopy, the pathognomonic circumferential hyperpigmented band of the peripheral retina was totally absent in two patients.

**Conclusion:** This report highlights the high phenotypic variability of autosomal dominant vitreoretinopathies, which may be misdiagnosed, especially in advanced forms with severe generalized photoreceptor dysfunction mimicking retinitis pigmentosa. Targeted next-generation sequencing can contribute to the proper clinical diagnosis, especially in case of atypical phenotypic features of autosomal dominant vitreoretinopathies.

RETINA 0:1–12, 2018

---

Autosomal dominant vitreoretinopathies (ADVIRC) is an extremely rare condition that was first described by Kaufman et al in 1982.<sup>1</sup> It is characterized by an autosomal dominant inheritance pattern, peripheral chorioretinal atrophy with retinal circumferential hyperpigmented band, tiny white pre-retinal opacities, fibrillar vitreous condensation, and blood-retinal barrier breakdown with retinal neovascularization.<sup>1,2</sup> An association with anterior segment abnormalities is frequent, including high hyperopia, angle-closure glaucoma, microcornea, microphthalmia, and presenile cataract<sup>3–5</sup> (Table 1).

Subjects affected with ADVIRC are classically asymptomatic during the first two decades of life unlike most cases of rod-cone or cone-rod dystrophies. Night vision disturbances, photophobia, and visual field abnormalities appear during adulthood with

a slow disease progression. Visual loss is usually related to early macular edema, vitreous hemorrhage, or acute angle-closure glaucoma. More recent studies reported progressive macular dysfunction with macular atrophy as a late manifestation of the disease.<sup>5,6</sup>

In 2004, Yardley et al were the first to identify *Bestrophin 1* (*BEST1*) mutations in five families presenting with ADVIRC. *BEST1* encodes a 585 amino acid transmembrane protein expressed in retinal pigment epithelium (RPE) cells.<sup>3,7</sup> Four missense mutations [p.(V86M), p.(V239M), p.(Y236C),<sup>3</sup> and p.(V235A)<sup>8</sup>] have been reported so far in association with ADVIRC. These mutations are believed to affect pre-mRNA splicing leading to in-frame deletion, unlike those underlying autosomal dominant Best macular dystrophy or autosomal recessive bestrophinopathy.<sup>3</sup>

Another entity called Microcornea-Rod cone dystrophy-Cataract-Posterior staphyloma (MRCS) is characterized by microcornea, rod-cone dystrophy, cataract, and posterior staphyloma. First described by Reddy et al in 2003, it presents some similarities with ADVIRC and has also been associated with mutations in *BEST1*. Given the resemblance between these two entities, it could be assumed that MRCS and ADVIRC are a continuum, MRCS being associated with a more severe phenotype.<sup>9</sup>

**Methods**

Here, we describe the cases of five patients with an atypical phenotype, for whom ADVIRC was retrospectively diagnosed on genetic results using targeted next-generation sequencing. For these patients, a diagnosis of cone-rod or rod-cone dystrophy was initially suspected, based on the clinical presentation. Targeted next-generation sequencing using a panel of 123 genes associated with inherited retinal diseases<sup>10</sup> led to the identification of a heterozygous missense mutations in *BEST1*: Patients 1, 2, 4, and 5 (family F2675, CIC05272 III-4 and CIC05537 III-7; family F4434 III-1, CIC07935 and CIC07936 III-2) were found heterozygous for c.256G>A, p.(Val86Met), whereas Patient 3 was heterozygous for c.715G>A p.(Val239Met) (family F614 CIC00989 III-3). These mutations had previously been reported underlying ADVIRC.<sup>3</sup> Patients did not carry pathogenic mutations in any of the other 122 genes tested in the panel,<sup>10</sup> including genes known to be mutated in autosomal dominant rod-cone and cone-rod dystrophies (<http://www.sph.uth.tmc.edu/Retnet/>).

Subsequently, we retrospectively reviewed the clinical charts of the five patients in light of these genetic results. Analysis was based on functional and

From the \*Fondation Ophtalmologique Adolphe de Rothschild, Paris, France; †Centre Hospitalier National d’Ophtalmologie des Quinze-Vingts, DHUSight Restore, INSERM-DGOS CIC 1423, Paris, France; ‡Académie des Sciences-Institut de France, Paris, France; §Sorbonne Universités, UPMC Univ Paris 06, INSERM U968, CNRS UMR\_7210, Institut de la Vision, Paris, France; ¶Department of Ophthalmology, The University of Pittsburgh School of Medicine, Pittsburgh, Pennsylvania; and \*\*Institute of Ophthalmology, University College of London, London, United Kingdom.

Supported by Fondation Voir et Entendre (C. Zeitz), Prix Dalloz for “La recherche en ophtalmologie” (C. Zeitz), LABEX LIFE-SENSES (reference ANR-10-LABX-65) supported by French state funds managed by the Agence Nationale de la Recherche within the Investissements d’Avenir program (ANR-11-IDEX-0004-0), Fondation Fighting Blindness center grant (C-CMM-0907-0428-INSERM04), and Prix de la Fondation de l’Œil (I. Audo).

None of the authors has any conflicting interests to disclose.

Reprint requests: Isabelle Audo, MD, PhD, Department of Genetics, INSERM, UMR\_S968, CNRS, UMR\_7210, UPMC Univ Paris 06, Institut de la Vision, 17 Rue Moreau, F-75012 Paris, France; e-mail: isabelle.audo@inserm.fr

Table 1. Phenotype of the five patients according to the reported classical findings of ADVIRC.

|   | Family 2675  |                                 | Family 614                      |                                 | Family 4434   |  |
|---|--|---------------------------------|---------------------------------|---------------------------------|---|--|
|   | Patient 1<br>CIC05537,<br>III-4  | Patient 2<br>CIC05272,<br>III-7 | Patient 3<br>CIC00989,<br>III-3 | Patient 4<br>CIC07935,<br>III-1 | Patient 5<br>CIC07936,<br>III-2                         |  |
| Classic Reported Findings <sup>1-5</sup>  |  |                                 |                                 |                                 |   |  |
| Autosomal dominant inheritance pattern  | +  | +                               | +                               | +                               | +   |  |
| Retinal circumferential hyperpigmented band   | +  | -                               | +                               | +                               | -   |  |
| Fibrillar vitreous condensation   | -  | +                               | -                               | -                               | -   |  |
| Tiny white preretinal opacities   | -  | -                               | -                               | -                               | -   |  |
| Blood-retinal barrier breakdown with retinal neovascularization   | -  | -                               | -                               | -                               | -   |  |
| Anterior segment abnormalities: high hyperopia, angle-closure glaucoma, microcornea, microphthalmia, and presenile cataract | + (congenital cataract, high hyperopia secondary to bilateral aphakia) | -                               | -                               | + (angle-closure glaucoma)      | + (narrowed angle treated by bilateral laser iridotomy) |  |

structural data, including best-corrected visual acuity using the Early Treatment Diabetic Retinopathy Study chart, slit-lamp examination of the anterior chamber, color vision test (Lanthony standard and desaturated 15 Hue), visual field test (Goldmann kinetic perimetry), retinophotography (CR1; Canon, Tokyo, Japan), short- and near-infrared wavelength autofluorescence fundus imaging, enhanced depth imaging spectral domain optical coherence tomography (EDI SD-OCT) (HRAII-Spectralis OCT; Heidelberg Engineering, Dossenheim, Germany), full-field electroretinogram (ffERG, Espion, Diagnosys),<sup>11</sup> and multifocal ERG (mfERG, Veris II, EDI)<sup>12</sup> according to the International Society for Clinical Electrophysiology of Vision (ISCEV) standards. Electrooculogram (EOG, WIN 7000C, Metrovision) was performed only in patients with moderate alterations of ffERG, when possible.

**Results**

The first two cases were two sisters from the same family (F2675) with a history of autosomal dominant uncharacterized retinal dystrophy.

*Case 1 (CIC05537, F2675 III-4)*

Patient 1 was a 49-year-old woman with a history of chronic open-angle glaucoma and a diagnosis of retinitis pigmentosa made when she was 23 years

old. She was complaining of night blindness, photophobia, and decreased central vision since early adulthood. Family history revealed similar cases with autosomal dominant inheritance pattern (Figure 1 top). Visual acuity was 20/80 with +17 for the right eye and <20/800 with +18 for the left eye. Slit-lamp examination revealed bilateral aphakia secondary to cataract surgery followed by explanation because of posterior intraocular lens luxation 20 years ago. Goldmann kinetic perimetry showed severe constriction of the peripheral visual field sparing the central 30° on the binocular III4e stimulus. Color vision testing revealed a tritan defect in the right eye, and could not be performed in the left eye because of the low vision (Figure 2 top left).

Full-field ERG and mfERG showed undetectable responses from background noise in both scotopic and photopic conditions (Figure 3 top left, Figure 4 top left) in keeping with severe generalized rod-cone dysfunction. For this reason, EOG, which depends on both photoreceptor and RPE function, was not performed.

Fundus examination of the posterior pole showed bilateral RPE changes in the peripapillary and macular regions. Examination of the peripheral retina revealed circumferential mottled pigmentation, distinct from intraretinal bone spicules. Fundus autofluorescence imaging revealed a hypoautofluorescent macular lesion surrounded by hyperautofluorescent borders on short- and near-infrared wavelength autofluorescence. On

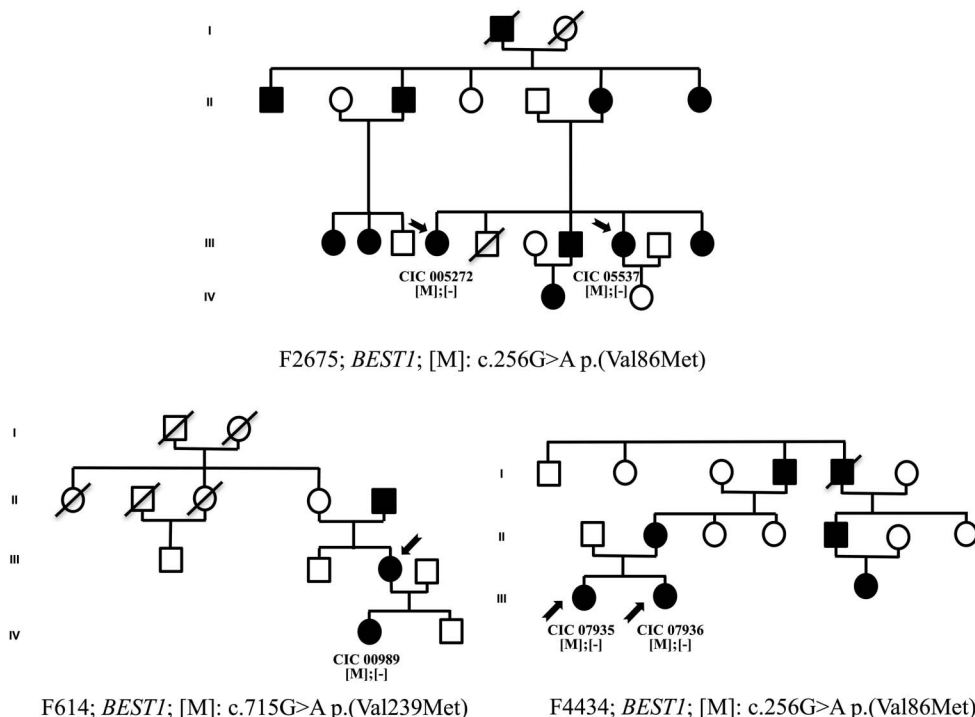


**Fig. 1.** Family tree for: F2675: Patients 1 (CIC05537) and 2 (CIC05272, F2675 III-7) (Top). F614: Patient 3 (CIC00989, F614 III-3) (Bottom left). F4434: Patients 4 (CIC07935, F4434 III-1) and 5 (CIC07936, F4434 III-2) (Bottom right). The disease displays an autosomal dominant inheritance pattern, with vertical transmission in the family, with male and female equally affected.

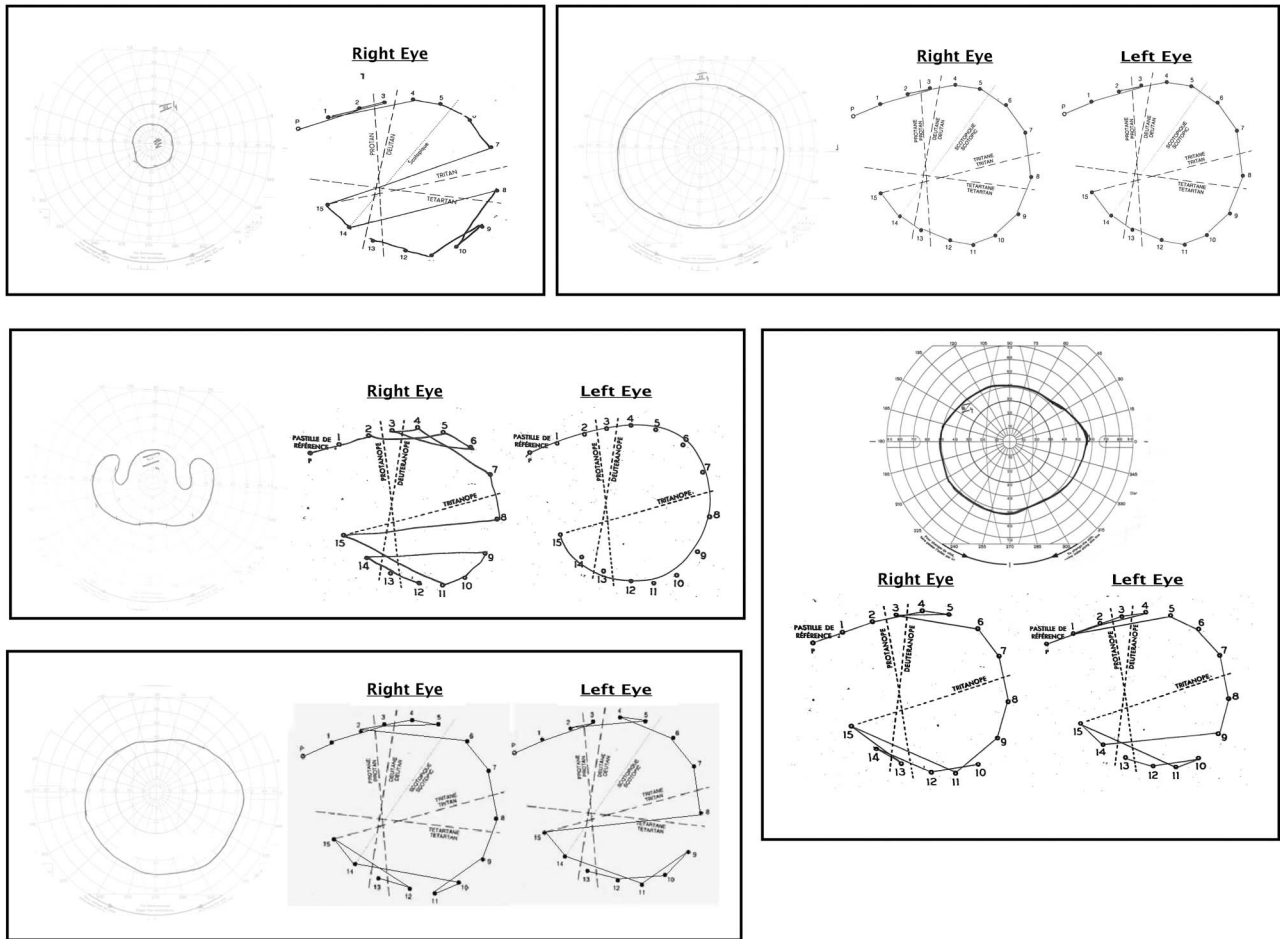


**Fig. 2.** CIC05537, F2675 III-4 Goldmann kinetic perimetry and color vision Lanthony 15 Hue test. Goldmann kinetic perimetry shows severe bilateral constriction of the peripheral visual field sparing the central 30° on the binocular III4e stimulus. Lanthony standard 15 Hue reveals a tritan defect in the right eye, and was not performed in the left eye because of the low vision (Top left). CIC05272, F2675 III-7 Goldmann kinetic perimetry showed a moderate constriction of the peripheral visual field on the binocular III4e stimulus. Lanthony desaturated 15 Hue is normal in both eyes (Top right). CIC00989, F614 III-3 Goldmann kinetic perimetry shows moderate constriction of peripheral isopters. Lanthony saturated 15 Hue reveals a tritan defect for the right eye and is normal for the left eye (Middle left). CIC07935, F4434 III-1 Goldmann kinetic perimetry shows mild constriction of the peripheral visual field extending from 110° horizontal to 100° vertical on the binocular III4e stimulus. Lanthony desaturated 15 Hue reveals a tritan defect in both eyes (Bottom left). CIC07936, F4434 III-2 Goldmann kinetic perimetry showed moderate constriction of the peripheral visual field extending from 100° horizontal to 90° vertical on the binocular III4e stimulus. Desaturated 15 Hue Lanthony revealed few errors in the tritan axis in both eyes (Middle right).

SD-OCT, the outer hyperreflective bands and outer nuclear layer were disrupted in the macular region with choroidal thinning and hyperreflectivity through window defect (Figure 5).

#### Case 2 (CIC05272, F2675 III-7)

Patient 2 was the 60-year-old elder sister of Patient 1 (Figure 1 Top). She was complaining of mild light sensitivity. Visual acuity was 20/32 with  $-0.25$  ( $-1.25$ ) 90° for the right eye and 20/25 with  $-0.50$  ( $-1.25$ ) 75° for the left eye. Slit-lamp examination showed bilateral pseudophakia with no abnormality of the anterior chamber. Lanthony desaturated 15 Hue was normal in both eyes. Goldmann kinetic peri-

metry showed a moderate constriction of the peripheral visual field on the binocular III4e stimulus (Figure 2 top right).

Full-field ERG revealed reduced and delayed responses predominant under photopic conditions in keeping with generalized cone-rod dysfunction (Figure 3 top middle). Multifocal ERG was unfortunately contaminated by artifacts, the patient experiencing difficulties to maintain a stable fixation, and revealed preservation of some of the responses to the central hexagons (Figure 4 top middle). Electrooculogram could unfortunately not be performed for this patient who did not want further testing.

Fundus examination was within normal limit, although of pale appearance with fibrillar vitreous

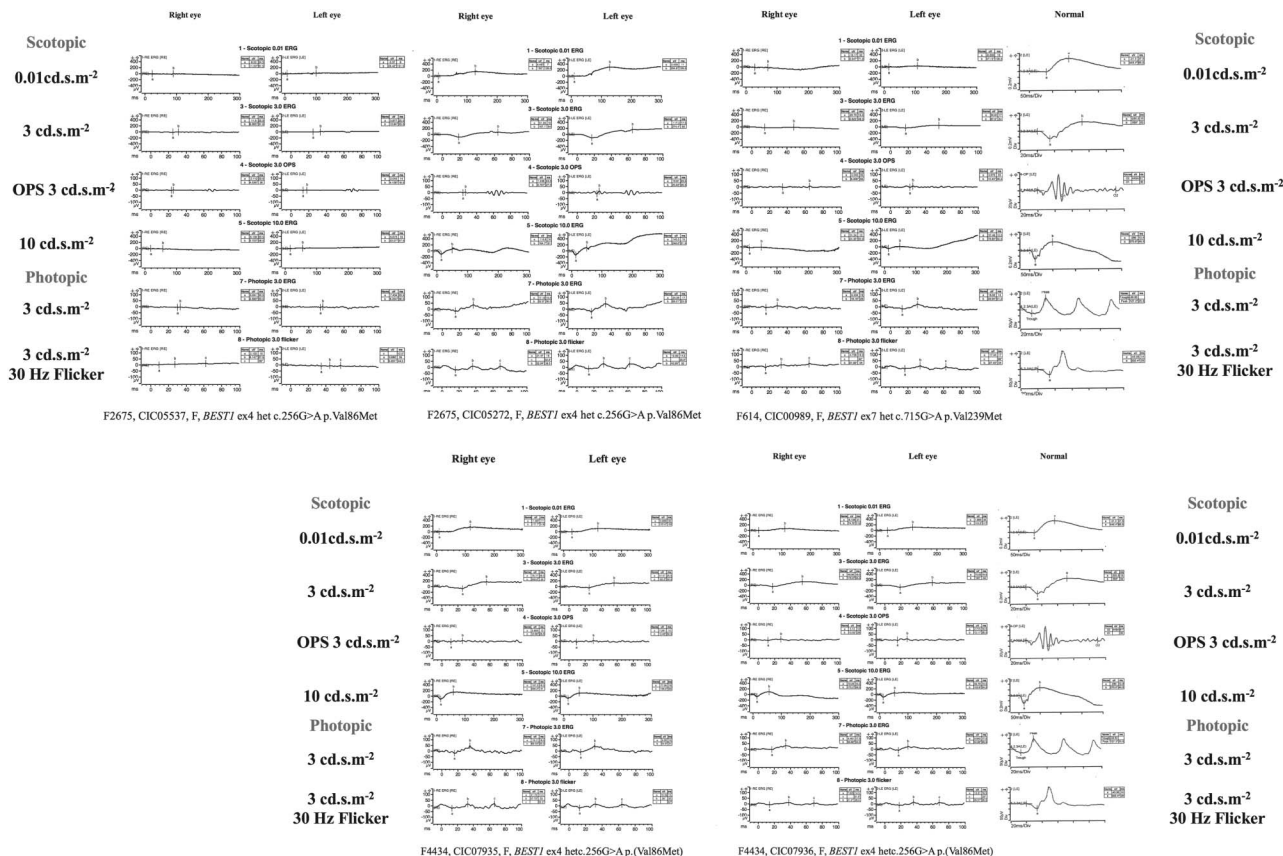


**Fig. 3.** CIC05537, F2675 III-4 full-field ERG shows undetectable response from background noise in both scotopic and photopic conditions in keeping with severe generalized rod-cone dysfunction (Top left). CIC05272, F2675 III-7 full-field ERG reveals reduced and delayed responses predominant under photopic conditions in keeping with generalized cone-rod dysfunction (Top middle). CIC00989, F614 III-3 full-field ERG shows some asymmetry between both eyes, responses from the left eyes being better preserved than those of the right eye. On the right, scotopic responses are undetectable from background noise, whereas only a hint of photopic responses is present. On the left, both scotopic and photopic responses are reduced in amplitude and delayed, with a better preservation of photopic than scotopic amplitudes. These results are in keeping with generalized rod-cone dysfunction more marked on the right than the left (Top right). CIC07935, F4434 III-1 full-field ERG shows reduced and delayed responses predominant under scotopic conditions in keeping with generalized rod-cone dysfunction (Bottom left). CIC07936, F4434 III-2 full-field ERG shows marked reduction of responses predominant under scotopic conditions in keeping with severe generalized rod-cone dysfunction (Bottom right).

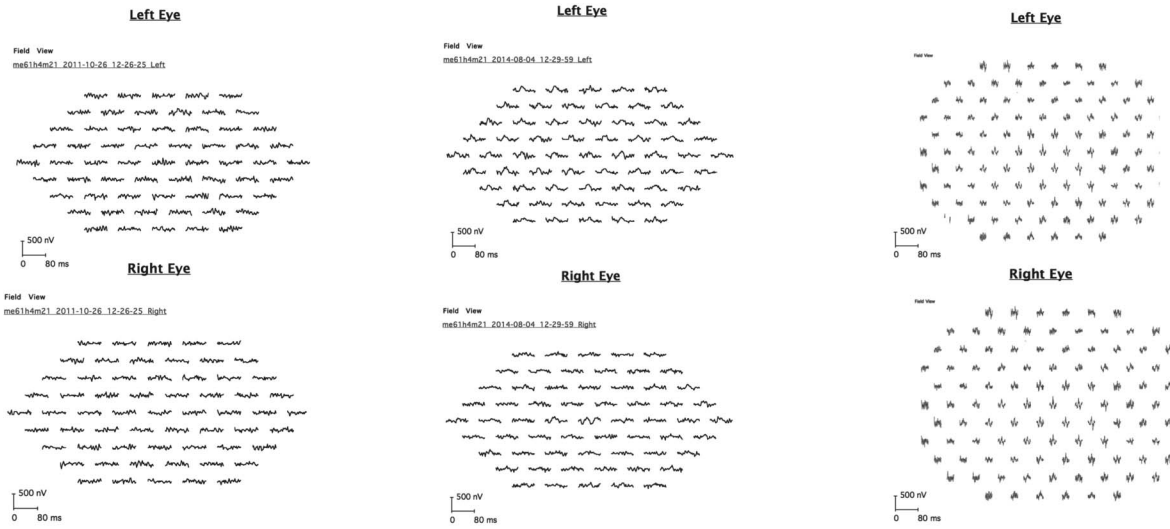
condensation hampering the quality of short-wavelength autofluorescence. Spectral domain OCT showed a granular appearance of the interdigitation and ellipsoid zones in the macular region with focal disruption of foveal hyperreflective bands and vitreomacular traction in the left eye (Figure 6).

*Case 3 (CIC00989, F614 III-3)*

Patient 3 was a 62-year-old female patient who complained about decreased central vision, photophobia, and night blindness since childhood. She was diagnosed with retinitis pigmentosa when she was 5 years old. Family history revealed similar cases with an autosomal dominant inheritance pattern (Figure 1 bottom left). Visual acuity was 20/100 with  $-4.50$  ( $-2.00$ )  $100^\circ$  for the right eye and 20/50 with  $-3.50$  ( $-1.25$ )  $85^\circ$  for the left eye. Slit-lamp examination showed bilateral corticonuclear cataract with no

other abnormality of the anterior chamber. Color vision testing revealed a tritan defect for the right eye and was normal for the left eye. Goldmann kinetic perimetry showed moderate constriction of peripheral isopters (Figure 2 middle left).

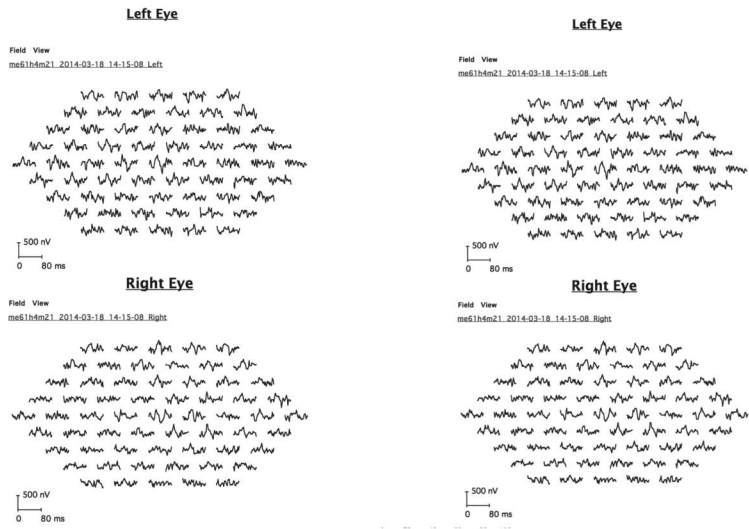
Full-field ERG showed some asymmetry between both eyes, responses from the left eyes being better preserved than those of the right eye. On the right, scotopic responses were undetectable from background noise, whereas only a hint of photopic responses was present. On the left, both scotopic and photopic responses were reduced in amplitude and delayed, with a better preservation of photopic than scotopic amplitudes. These results were in keeping with generalized rod-cone dysfunction more marked on the right than the left. This functional asymmetry is correlated with more severe structural alteration of the outer retina in the right eye (Figure 3 top left). Multifocal ERG,



F2675, CIC05537, F, *BEST1* ex4 het c.256G>A p.Val86Met

F2675, CIC05272, F, *BEST1* ex4 het c.256G>A p.Val86Met

F614, CIC00989, F, *BEST1* ex7 het c.715G>A p.Val239Met



F4434, CIC07935, F, *BEST1* ex4 het c.256G>A p.(Val86Met)

F4434, CIC07936, F, *BEST1* ex4 het c.256G>A p.(Val86Met)

**Fig. 4.** CIC05537, F2675 III-4 multifocal ERG shows undetectable response from background noise in keeping with severe macular dysfunction (Top left). CIC05272, F2675 III-7 multifocal ERG is unfortunately contaminated by artifacts, the patient experiencing difficulties to maintain a stable fixation, and reveals preservation of some of the responses to the central hexagons (Top middle). CIC00989, F614 III-3 multifocal ERG, although contaminated with electrical artifact, reveals relatively preserved responses to the peripheral responses in keeping with a relatively preserved macular cone function (Top right). CIC07935, F4434 III-1 multifocal ERG is unfortunately contaminated by artifacts, the patient experiencing difficulties to maintain a stable fixation, and was not interpretable (Bottom left). CIC07936, F4434 III-2 multifocal ERG, although contaminated with electrical artifact, reveals relatively preserved responses to central hexagons compared with the peripheral responses in keeping with a relatively preserved macular cone function (Bottom right).

although contaminated with electrical artifacts, revealed relatively preserved responses to central hexagons compared with the peripheral responses in keeping with a relatively preserved macular cone function (Figure 4 top left).

Fundus examination was normal at the posterior pole. Examination of the peripheral retina revealed bilateral circumferential annular coarse pigment migration. Short-wavelength and near-infrared auto-

fluorescence revealed a diffuse irregular increase of autofluorescence at the posterior pole with a decreased autofluorescence inferiorly and in the far periphery. These changes were not seen on fundoscopy. On SD-OCT, the outer hyperreflective bands and the outer nuclear layer were diffusely disrupted in the right eye with a relative foveal sparing in the left in keeping with the relatively well-preserved visual acuity on this side (Figure 7).

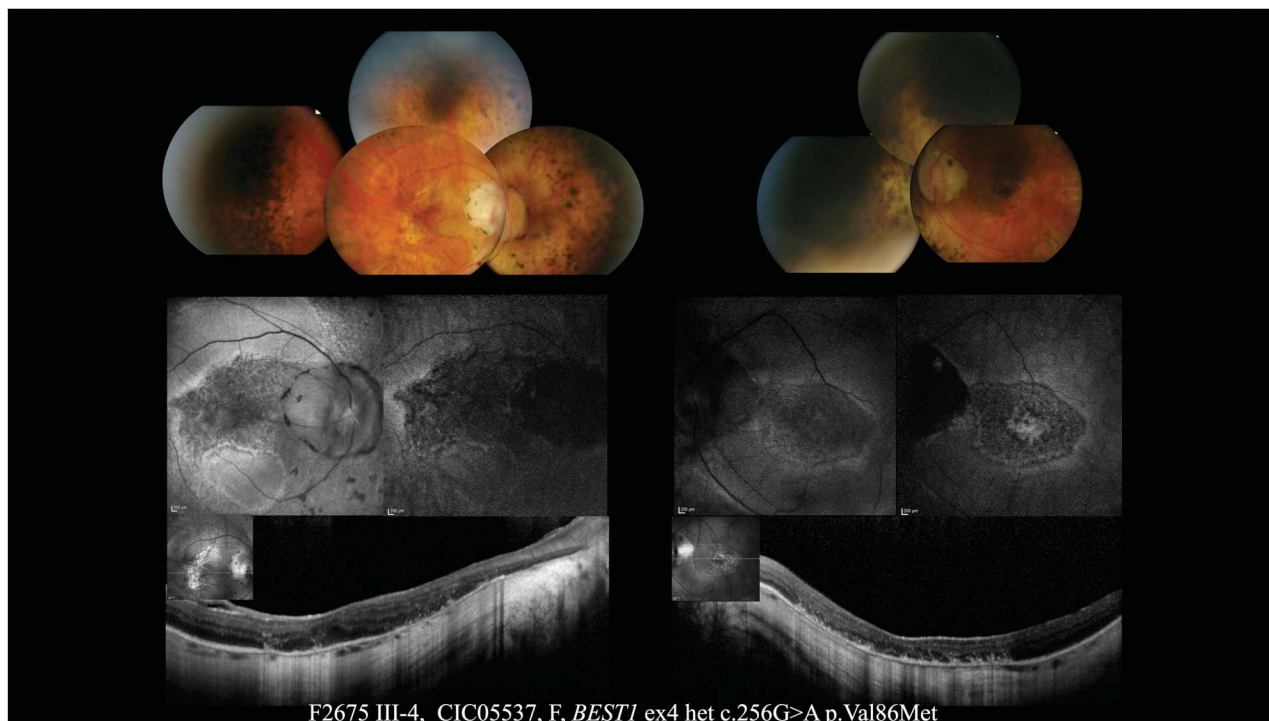


**Fig. 5.** Multimodal retinal imaging of Patient 1, a 49-year-old woman (F2675 III-4, CIC05537) carrying the heterozygous c.256 G>A; p.Val86Met *BEST1* mutation. Fundoscopy of the posterior pole (Top) shows bilateral RPE changes in the peripapillary and macular regions. Peripheral retina reveals circumferential mottled pigmentation, distinct from intraretinal bone spicules. Fundus autofluorescence imaging reveals a hypoautofluorescent macular lesion surrounded by hyperautofluorescent borders on short-wavelength (Middle left) and near-infrared (Middle right) autofluorescence. On SD-OCT (Bottom), the outer hyperreflective bands and outer nuclear layer are disrupted in the macular region with choroidal thinning and hyperreflectivity through window defect.

The last two cases were two sisters from the same family (F4434) with a history of autosomal dominant uncharacterized retinal dystrophy.

#### Case 4 (CIC07935, F4434 III-1)

Patient 4 was a 71-year-old female patient with a history of acute angle-closure glaucoma of the left eye treated with bilateral laser iridotomy. She complained of night blindness, photophobia, and decreased vision since adulthood. She was diagnosed with late-onset generalized retinal dystrophy a few years earlier. Family history revealed similar cases with an autosomal dominant inheritance pattern (Figure 1 bottom right). Visual acuity was 20/63 with +1.75 (−0.75) 50° for the right eye and 20/32 with −1.25 (−1) 140° for the left eye. Slit-lamp examination revealed corticonuclear cataract of the right eye and pseudophakia of the left eye. Goldmann kinetic perimetry showed mild constriction of the peripheral visual field extending from 110° horizontal to 100° vertical on the binocular III4e stimulus. Lanthony desaturated 15 Hue revealed a tritan defect in both eyes (Figure 2 bottom left).

Full-field ERG showed reduced and delayed responses predominant under scotopic conditions in

keeping with generalized rod-cone dysfunction (Figure 3 bottom left). Multifocal ERG was unfortunately contaminated by artifacts, the patient experiencing difficulties to maintain a stable fixation, and was not interpretable (Figure 4 bottom left). Electrooculogram revealed severely reduced light peak with decreased Arden ratio (125% for the right eye, 145% for the left eye), in keeping with generalized dysfunction of the RPE (Figure 8).

Fundus examination was normal at the posterior pole. Examination of the extreme peripheral retina revealed bilateral circumferential annular coarse pigment migration. Short-wavelength and near-infrared autofluorescence revealed bilateral peripapillary hypoautofluorescence and subtle alterations in the macular region. On SD-OCT, the outer hyperreflective bands and the outer nuclear layer were preserved outside the peripapillary region. Spectral domain OCT also revealed vitreomacular traction in the temporomacular region of the right eye and a macular epiretinal membrane in the left eye (Figure 9).

#### Case 5 (CIC07936, F4434 III-2)

Patient 5 was the 66-year-old younger sister of Patient 4 (Figure 1 bottom right).



**Fig. 6.** Multimodal retinal imaging of Patient 2, a 60-year-old woman (F2675 III-7, CIC05272) carrying the heterozygous c.256 G>A p.Val86Met *BEST1* mutation. Fundoscopy (Top) is within normal limit, although of pale appearance with fibrillar vitreous condensation hampering the quality of short-wavelength (Middle left) and near-infrared (Middle right) autofluorescence. Spectral domain OCT (Bottom) shows a granular appearance of the interdigitation and ellipsoid zones in the macular region with focal disruption of foveal hyperreflective bands and vitreomacular traction in the left eye.

She was complaining of night blindness, photophobia, and decreased vision since adulthood. Visual acuity was 20/80 in both eyes with  $-7$  ( $-1.75$ )  $100^\circ$  for the right eye and  $-6$  ( $-2.25$ )  $80^\circ$  for the left eye. Slit-lamp examination revealed bilateral corticonuclear cataract and narrowed angle treated by bilateral laser iridotomy. Goldmann kinetic perimetry showed moderate constriction of the peripheral visual field extending from  $100^\circ$  horizontal to  $90^\circ$  vertical on the binocular III4e stimulus. Lanthony desaturated 15 Hue revealed few errors in the tritan axis in both eyes (Figure 2 middle right).

Full-field ERG showed marked reduction of responses predominant under scotopic conditions in keeping with severe generalized rod-cone dysfunction. Multifocal ERG, although contaminated with electrical artifact, revealed relatively preserved responses to central hexagons compared with the peripheral responses in keeping with a relatively preserved macular cone function (Figure 3 bottom right).

Fundus examination of the posterior pole showed chorioretinal atrophic changes in the peripapillary region and the inferonasal mild periphery of the retina. No pigmentary changes were observed in the peripheral retina. Short-wavelength and near-infrared autofluorescence revealed hypoautofluorescence patches of the peripapillary region and the peripheral retina sparing the

macular region. On SD-OCT, the outer hyperreflective bands were disrupted in the macular region with foveal sparing, choroidal thinning, and hyperreflectivity through window defect. Spectral domain OCT also revealed bilateral macular epiretinal membranes with a foveal cyst in the left eye (Figure 10).

## Discussion

Autosomal dominant vitreoretinchoroidopathy is an extremely rare, autosomal dominantly inherited retinal dystrophy that is attributed to mutations in *BEST1*. The gene encodes a transmembrane protein, bestrophin, localized at the basolateral plasma membrane of RPE cells where it acts as an anion channel and plays a role in intracellular calcium homeostasis.<sup>9</sup> The clinical phenotype of ADVIRC is distinct from other bestrophinopathies, such as Best vitelliform macular dystrophy or autosomal recessive bestrophinopathy, also associated with mutations in *BEST1*. Known mutations in ADVIRC are hypothesized to result in altered splicing of *BEST1* leading to either in-frame deletions or duplications.<sup>3,5,8</sup>

This might account for the distinct ocular phenotype and high incidence of developmental anomalies in



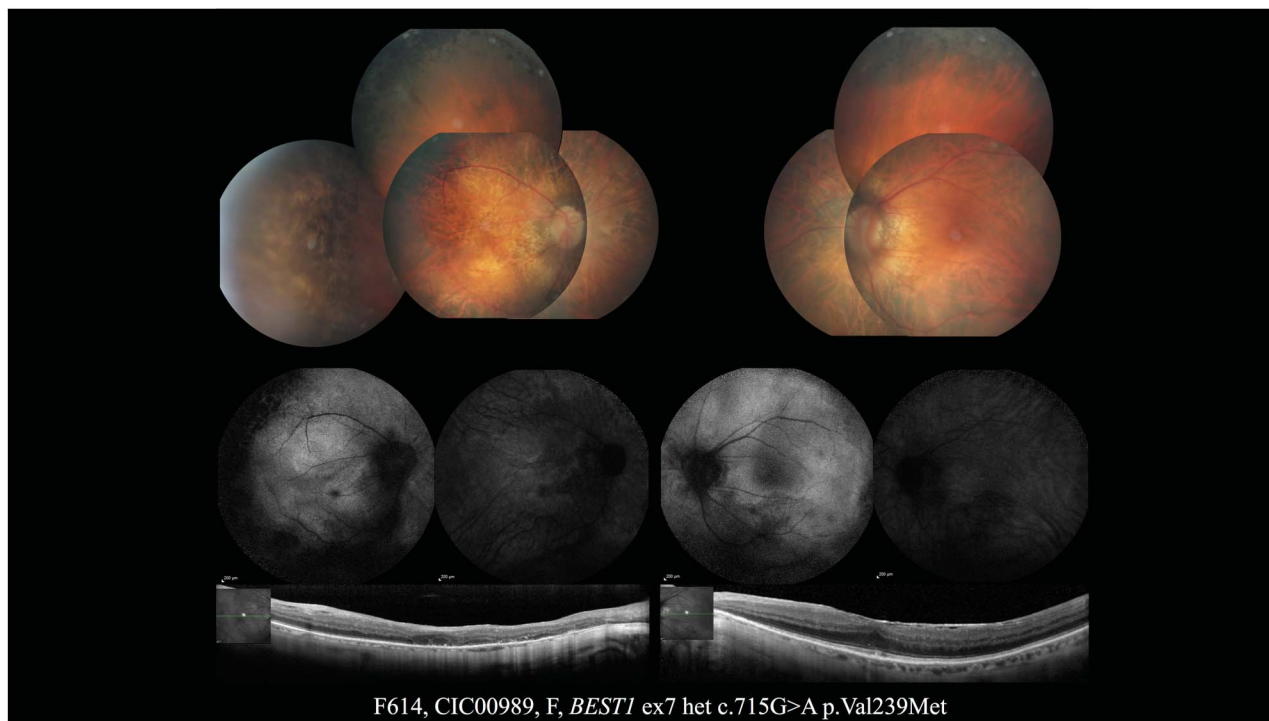
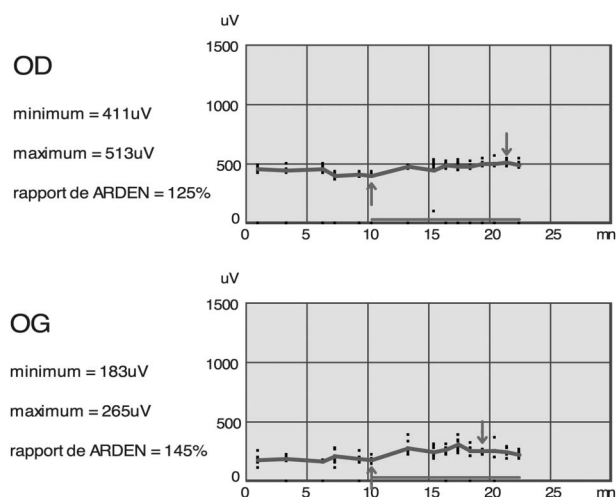


**Fig. 7.** Multimodal retinal imaging of Patient 3, a 62-year-old woman (F614 III-3, CIC00989) carrying the heterozygous c.715G>A p.Val239Met *BEST1* mutation. Fundoscopy (Top) is normal at the posterior pole. Peripheral retina reveals bilateral circumferential annular coarse pigment migration. Short-wavelength (Middle left) and near-infrared (Middle right) autofluorescence reveals a diffuse irregular increase of autofluorescence at the posterior pole with a decreased autofluorescence inferiorly and in the far periphery. On SD-OCT (Bottom), the outer hyperreflective bands and the outer nuclear layer are diffusely disrupted in the right eye with a relative foveal sparing in the left in keeping with the relatively well-preserved visual acuity on this side. An epimacular membrane is also present in the left eye.

ADVIRC.<sup>4</sup> Only, Chen et al recently reported a new missense mutation underlying ADVIRC [c.248G>A; p.(Gly83Asp)], although involving the first base of exon 4 of *BEST1* for which in vitro splicing assays



F4434, CIC07935, F, *BEST1* ex4 het c.256G>A p.(Val86Met)

**Fig. 8.** CIC07935, F4434 III-1 EOG reveals severely reduced light peak with decreased Arden ratio (125% for the right eye, 145% for the left eye), in keeping with generalized dysfunction of the RPE.

did not demonstrate a clear effect on splicing.<sup>5</sup> A recent study using induced pluripotent stem cells suggested a mislocalization of *BEST1* to the apical membrane of RPE cells in the peripheral retina during the early developmental stage which may play a role in the pathology.<sup>7</sup> Further studies are needed to determine whether in vivo splicing alterations can account for the observed ADVIRC phenotype.<sup>5,7</sup>

As previously outlined by Vincent et al,<sup>4</sup> the three cases reported here emphasize the high interfamilial and intrafamilial phenotypic variability of ADVIRC.<sup>13</sup> Clinical presentation varies in a same family (Figure 1 top) from characteristic features of ADVIRC (F2675 III-4) to atypical presentation (F2675 III-7), making the diagnosis in this latter case difficult (Table 1).

The classic peripheral band of chorioretinal hyperpigmentation between the equator and the ora serrata is typically considered a constant feature of ADVIRC.<sup>4</sup> However, caution must be taken because Patient 2 demonstrates that peripheral pigmentation can be totally missing (Table 1). At the late stage of the disease, hyperpigmented band progressively reaches the posterior pole and may also become less distinguishable, leading to chorioretinal atrophy, as shown in Patient 5.<sup>13</sup>

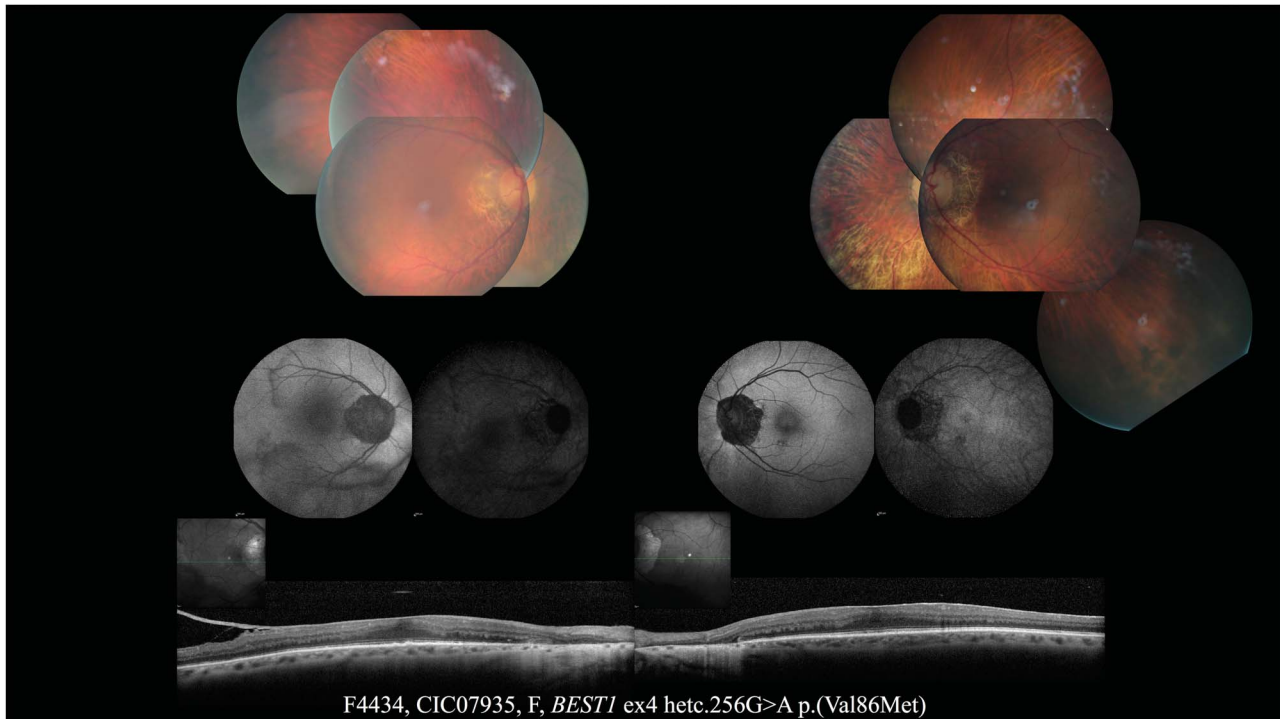


**Fig. 9.** Multimodal retinal imaging of Patient 4, a 71-year-old woman (F4434 III-1, CIC07935) carrying the heterozygous c.256 G>A; p.Val86Met *BEST1* mutation. Fundoscopy (Top) is normal at the posterior pole. Annular coarse pigment migration is visible in the nasal inferior part of the extreme peripheral retina on retinophotography. Short-wavelength (Middle left) and near-infrared (Middle right) autofluorescence revealed bilateral peripapillary hypoautofluorescence and subtle alterations in the macular region. On SD-OCT (Bottom), the outer hyperreflective bands and the outer nuclear layer were preserved outside the peripapillary region. Spectral domain OCT also revealed vitreomacular traction in the temporomacular region of the right eye and a macular epiretinal membrane of the left eye.

Anterior segment abnormalities are also not constant, as reported by Kellner et al<sup>14</sup> in a family carrying the c.256G>A mutation. None of our five patients had microcornea, microphthalmia, or nanophthalmia. Refraction was not specific, varying from high hyperopia to high myopia. Presenile cataract was removed in 5/10 eyes. Two patients had narrowed angle with history of unilateral acute angle-closure glaucoma for one patient. Both of them were treated by bilateral laser iridotomy (Table 1).

Electrophysiological findings are not specific of ADVIRC so that erroneous diagnosis of rod-cone or cone-rod dystrophy can be delivered, as reported in the previous cases. According to Lafaut et al, ffERG shows variable results from normal or subnormal to severely reduced rod and/or cone amplitude responses with normal or only slightly delayed implicit times. Full-field ERG amplitudes are usually normal during the first decade of life and tend to decrease with aging.<sup>15</sup> Electrooculogram was not performed in 4/5 subjects because of the severe retinal dysfunction (3/5, F2675 III-4, F614 III-3, F4434 III-2) and the misdiagnosis of ADVIRC (1/5, F2675 III-7). According to Han et al,<sup>16</sup> EOG is classically abnormal at the early phase of the disease with markedly reduced Arden

ratio, as confirmed by Patient 4 and as usually observed in *BEST1*-related diseases. Electrooculogram can also rarely be normal.<sup>16,17</sup>

Autosomal dominant vitreoretinopathy is an extremely rare disease that is not well recognized by clinicians. It is often mistaken for more frequent retinal dystrophies, especially at the late stage of the disease. Differential diagnoses that should be considered for ADVIRC are retinitis pigmentosa or rod-cone dystrophy, cone-rod dystrophy, and late-onset retinal dystrophy. If the pathognomonic peripheral hyperpigmented band is noticed at fundus examination, ADVIRC should be considered and *BEST1* genetic testing performed. Another clinical entity called autosomal dominant neovascular inflammatory vitreoretinopathy which is linked to *CAPN5* mutations should be distinguished from ADVIRC. Autosomal dominant neovascular inflammatory vitreoretinopathy is also an extremely rare disease with progressive photoreceptor degeneration and additional features including severe intraocular inflammation with retinal neovascularization, intraocular fibrosis, and retinal detachment, which are not found in patients with ADVIRC.<sup>18,19</sup> In case of high hyperopia, an alternative differential diagnosis for ADVIRC could be posterior

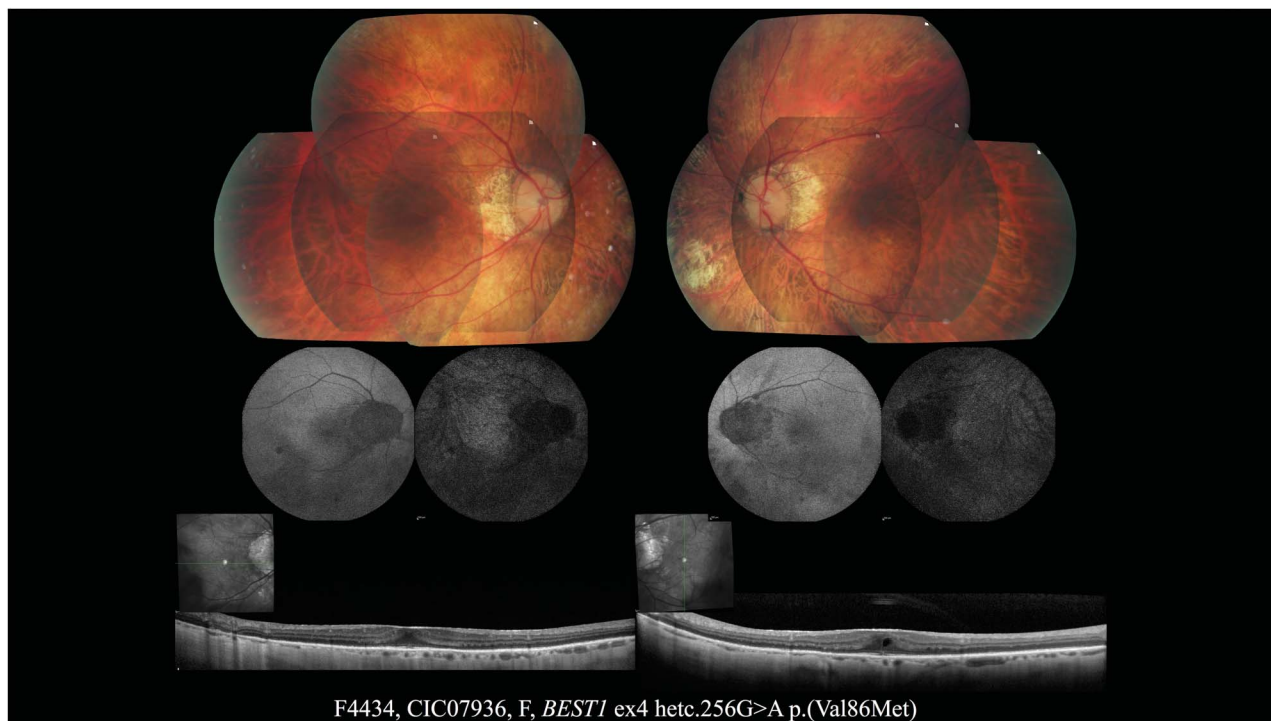


**Fig. 10.** Multimodal retinal imaging of Patient 5, a 66-year-old woman (F4434 III-2, CIC07936) carrying the heterozygous c.256G>A; p.Val86Met *BEST1* mutation. Fundoscopy of the posterior pole (Top) shows chorioretinal atrophic changes in the peripapillary region and the inferonasal mild periphery of the retina. No pigmentary changes are observed in the peripheral retina. Short-wavelength (Middle left) and near-infrared (Middle right) autofluorescence reveals hypoautofluorescence patches of the peripapillary region and the peripheral retina sparing the macular region. On SD-OCT (Bottom), the outer hyperreflective bands are disrupted in the macular region with foveal sparing, choroidal thinning, and hyperreflectivity through window defect. Spectral domain OCT also reveals bilateral macular epiretinal membrane with one foveal cystoid cyst in the left eye.

microphthalmia with retinitis pigmentosa and foveoschisis.<sup>20</sup> However, in the later case, the disorder is autosomal recessive, with retinal fold and foveoschisis unlike in ADVIRC.<sup>20</sup>

The visual prognosis of ADVIRC is considered to be less severe than rod-cone or cone-rod dystrophies. Nevertheless, long-term follow-up of first ADVIRC probands revealed macular involvement with progressive visual field constriction both leading to severe visual impairment in the late stage of the disease.<sup>6,14</sup> Acute angle-closure glaucoma is another severe complication of ADVIRC that should be detected systematically and may be prevented by laser iridotomy in at-risk patients.

### Conclusion

Autosomal dominant vitreoretinopathopathy is an extremely rare disease, which is often overlooked because of the high phenotypic variability, as reported here. To properly diagnose it, EOG should be part of the routine work-up providing that fERG responses are sufficiently preserved to relevantly interpret the EOG abnormalities as related to severe RPE dysfunction. Targeted next-generation sequencing can help for

retrospective clinical diagnosis, especially of atypical ADVIRC features. The latter diagnosis should be systematically considered in case of peripheral chorioretinal degeneration with a sharply demarcated band of hyperpigmentation and autosomal dominant inheritance. In such cases, it would be of interest to carefully examine retinal periphery and perform wide-field imaging, to detect this characteristic peripheral hyperpigmented band. A correct diagnosis of ADVIRC may have a significant impact in preventing potential acute angle-closure glaucoma by peripheral laser iridotomy in affected individuals with narrowed anterior chamber. A correct ADVIRC diagnosis is also essential in the perspective of future therapies, such as gene therapy and stem cell-derived RPE transplantation.<sup>9</sup>

**Key words:** ADVIRC, retinal dystrophy, bestrophin-1 gene, peripheral retinal hyperpigmentation, inherited retinal disease.

### Acknowledgments

The authors are thankful to the patients and family members participating in the study and to the clinical staff from the Centre d'Investigation Clinique CIC1438. DNA samples included in this study

originate from NeuroSensCol DNA bank (PI: J.-A.S., coPI the authors I.A., partner with Centre Hospitalier National d’Ophtalmologie des Quinze-Vingts, INSERM and CNRS).

### References

1. Kaufman SJ, Goldberg MF, Orth DH, et al. Autosomal dominant vitreoretinopathopathy. *Arch Ophthalmol* 1982;100:272–278.
2. Blair NP, Goldberg MF, Fishman GA, Salzano T. Autosomal dominant vitreoretinopathopathy (ADVIRC). *Br J Ophthalmol* 1984;68:2–9.
3. Yardley J, Leroy BP, Hart-Holden N, et al. Mutations of VMD2 splicing regulators cause nanophthalmos and autosomal dominant vitreoretinopathopathy (ADVIRC). *Invest Ophthalmol Vis Sci* 2004;45:3683–3689.
4. Vincent A, McAlister C, Vandenhoven C, Héon E. BEST1-related autosomal dominant vitreoretinopathopathy: a degenerative disease with a range of developmental ocular anomalies. *Eye Lond Engl* 2011;25:113–118.
5. Chen CJ, Kaufman S, Packo K, et al. Long-term macular changes in the first proband of autosomal dominant vitreoretinopathopathy (ADVIRC) due to a newly identified mutation in BEST1. *Ophthalmic Genet* 2016;37:102–108.
6. Chen CJ, Goldberg MF. Progressive cone dysfunction, geographic atrophy of the macula in late stage autosomal dominant vitreoretinopathopathy (ADVIRC). *Ophthalmic Genet* 2014. doi: 10.3109/13816810.2014.889171.
7. Carter DA, Smart MJK, Letton WVG, et al. Mislocalisation of BEST1 in iPSC-derived retinal pigment epithelial cells from a family with autosomal dominant vitreoretinopathopathy (ADVIRC). *Sci Rep* 2016;6:33792.
8. Burgess R, MacLaren RE, Davidson AE, et al. ADVIRC is caused by distinct mutations in BEST1 that alter pre-mRNA splicing. *J Med Genet* 2009;46:620–625.
9. Johnson AA, Guziewicz KE, Lee CJ, et al. Bestrophin 1 and retinal disease. *Prog Retin Eye Res* 2017;58:45–69.
10. Boulanger-Scemama E, El Shamieh S, Démontant V, et al. Next-generation sequencing applied to a large French cone and cone-rod dystrophy cohort: mutation spectrum and new genotype-phenotype correlation. *Orphanet J Rare Dis* 2015; 10:85.
11. McCulloch DL, Marmor MF, Brigell MG, et al. ISCEV Standard for full-field clinical electroretinography (2015 update). *Doc Ophthalmol Adv Ophthalmol* 2015;130:1–12.
12. Hood DC, Bach M, Brigell M, et al. ISCEV standard for clinical multifocal electroretinography (mfERG) (2011 edition). *Doc Ophthalmol Adv Ophthalmol* 2012;124:1–13.
13. François P, Puech B, Hache JC, Laffineur Q. Vitreoretinohoroidal heredo-dystrophy, microcornea, glaucoma and cataract. *J Fr Ophthalmol* 1993;16:29–40.
14. Kellner S, Stöhr H, Fiebig B, et al. Fundus autofluorescence and SD-OCT document rapid progression in autosomal dominant vitreoretinopathopathy (ADVIRC) associated with a c.256G > A mutation in BEST1. *Ophthalmic Genet* 2016; 37:201–208.
15. Lafaut BA, Loeys B, Leroy BP, et al. Clinical and electrophysiological findings in autosomal dominant vitreoretinopathopathy: report of a new pedigree. *Graefes Arch Clin Exp Ophthalmol* 2001;239:575–582.
16. Han DP, Lewandowski MF. Electro-oculography in autosomal dominant vitreoretinopathopathy. *Arch Ophthalmol* 1992; 110:1563–1567.
17. Kellner U, Jandek C, Kraus H, Foerster MH. Autosomal dominant vitreoretinopathopathy with normal electrooculogram in a German family. *Graefes Arch Clin Exp Ophthalmol* 1998; 236:109–114.
18. Mahajan VB, Skeie JM, Bassuk AG, et al. Calpain-5 mutations cause autoimmune uveitis, retinal neovascularization, and photoreceptor degeneration. *PLoS Genet* 2012;8: e1003001.
19. Bassuk AG, Yeh S, Wu S, et al. Structural modeling of a novel CAPN5 mutation that causes uveitis and neovascular retinal detachment. *PLoS One* 2015;10:e0122352.
20. Ayala-Ramirez R, Graue-Wiechers F, Robredo V, et al. A new autosomal recessive syndrome consisting of posterior microphthalmos, retinitis pigmentosa, foveoschisis, and optic disc drusen is caused by a MFRP gene mutation. *Mol Vis* 2006; 12:1483–1489.